Original Paper

Cellular Physiology and Biochemistry

Cell Physiol Biochem 2009;24:605-618

Accepted: October 08, 2009

Cholesterol Depletion of the Plasma Membrane Prevents Activation of the Epithelial Sodium Channel (ENaC) by SGK1

Bettina Krueger[1], Silke Haerteis[1], Limin Yang[1], Andrea Hartner[2], Robert Rauh[1], Christoph Korbmacher[1] and Alexei Diakov[1]

[1]Institut für Zelluläre und Molekulare Physiologie, [2]Kinder- und Jugendklinik des Universitätsklinikums Erlangen, Friedrich-Alexander-Universität Erlangen-Nürnberg

Key Words

Epithelial sodium channel (ENaC) • Serum- and glucocorticoid-induced kinase isoform 1 • Lipid raft • Methyl-β-cyclodextrin • Cholesterol • *Xenopus laevis* oocytes

Abstract

The lipid environment of the epithelial sodium channel (ENaC) and its possible association with so-called lipid rafts may be relevant to its function. The aim of our study was to confirm the association of ENaC with lipid rafts and to analyze the effect of cholesterol depletion of the plasma membrane by methyl-β-cyclodextrin (MβCD) on channel function and regulation. Using sucrose density gradient centrifugation we demonstrated that a significant portion of ENaC protein distributes to low density fractions thought to be typical lipid raft fractions. Importantly, cholesterol depletion of cell lysate by MβCD shifted ENaC to non-raft fractions of higher density. Live cell imaging demonstrated that treatment with MβCD largely reduced filipin staining over time, confirming cholesterol depletion of the plasma membrane. For electrophysiological studies intact oocytes were exposed to 20 mM MβCD for three hours. MβCD treatment had no consistent effect on baseline whole-cell ENaC currents. In addition to the typical single channel conductance of about 5 pS, subconductance states of ENaC were occasionally observed in patches from MβCD treated but not from control oocytes. Importantly, in outside-out patch clamp recordings the stimulatory effect of recombinant SGK1 in the pipette solution was essentially abolished in oocytes pretreated with MβCD. These results indicate that ENaC activation by cytosolic SGK1 is compromised by removing cholesterol from the plasma membrane. Thus, ENaC activation by SGK1 may require the presence of an intact lipid environment and/or of lipid rafts as signalling platform.

Introduction

The epithelial sodium channel (ENaC) is the rate limiting transport mechanism for sodium absorption in a number of epithelia [1-3]. To adjust channel activity to functional needs, the open probability of ENaC, its surface expression, its intracellular trafficking, and its *de novo* synthesis are highly regulated [2, 4]. Moreover, the function and regulation of ENaC may be modified by its lipid environment and by the channel's association with

KARGER

Fax +41 61 306 12 34
E-Mail karger@karger.ch
www.karger.com

1015-8987/09/0246-0605$26.00/0

Accessible online at:
www.karger.com/cpb

Prof. Dr. med. Christoph Korbmacher
Institut für Zelluläre und Molekulare Physiologie, Friedrich-Alexander-Universität Erlangen-Nürnberg, Waldstr. 6, D-91054 Erlangen (Germany)
Tel. +49-9131-8522301, Fax +49-9131-8522770
E-Mail christoph.korbmacher@physiologie2.med.uni-erlangen.de

so-called 'lipid rafts' [5-9].

Lipid rafts are microdomains in the cell membrane which are more highly ordered and less fluid than the bulk membrane [10-12]. In these membrane microdomains glycosphingolipids, sphingomyelin and cholesterol are clustered. Lipid rafts are thought to serve as dynamic assembly and sorting platforms for proteins on their way to the apical membrane and to allow sequestering of proteins in close proximity for functional interaction [13, 14]. Identification of lipid raft associated proteins is usually based on biochemical characteristics of these lipid-enriched domains: The insolubility of lipid rafts in nonionic detergents such as Triton X-100 at low temperatures and, the distribution to low buoyant density after gradient centrifugation [15]. Thus, detection of membrane proteins in low density fractions suggests that they are associated with lipid rafts. Depending on the detergent that is used, detergent resistant membranes of variable lipid composition can be separated and different proteins are associated with the membranes depending on their lipid environment [16]. Therefore, to define lipid rafts as detergent resistant membranes is problematic and most likely an oversimplification [17, 18]. Interestingly, a non-detergent method for membrane solubilization can also be used to separate lipid rafts by their low buoyant density from other microdomains of the membrane and some proteins were found to be specifically associated with these domains [16]. Several transporters and ion channels have been reported to be associated with lipid rafts. Examples are aquaporins [19], CFTR [20], N-type Ca^{2+} channels [21], NHE3 [22], NKCC2 [23], cardiac Na^+ channels [24, 25], and a broad range of K^+ channels (reviewed in [26]). For these channels and transporters, the intact lipid raft structure is thought to be important for proper function. This is usually concluded from the observation that their function can be disturbed by cholesterol depletion of the plasma membrane by methyl-β-cyclodextrin (MβCD), a treatment which is thought to destroy the integrity of lipid rafts [27].

In the distal nephron and distal colon the appropriate regulation of ENaC activity is of fundamental importance for the maintenance of body sodium balance and, therefore, for the long term regulation of arterial blood pressure [28, 29]. In these tissues, the most important hormone to stimulate ENaC activity is the mineralocorticoid aldosterone. The stimulatory effect of aldosterone involves a cascade of aldosterone-induced and aldosterone-repressed regulatory proteins which may need to be co-assembled in lipid rafts. The serum- and glucocorticoid-induced kinase isoform 1 (SGK1) [30] is an early aldosterone-induced gene which increases ENaC activity by complex mechanisms including the phosphorylation of Nedd4-2 and probably also a direct phosphorylation of the channel. Indeed, acute stimulation of ENaC activity by recombinant SGK1 in outside-out patches has been shown to depend on a serine residue in a putative SGK1 consensus motif in the C-terminus of the channel's α-subunit [31].

There is growing evidence that not only protein-protein interactions are important for ENaC regulation, but that the surrounding lipid composition also plays a role. For example, it has been reported that changes in temperature influence membrane lipid order and modulate ENaC activity. These effects suggest that a lipid-protein interaction is involved in ENaC regulation [9]. Moreover, ENaC expressed in A6 renal epithelial cells was found to be associated with lipid raft fractions in a buoyant density assay. Interestingly, this association appeared to be altered by pretreating the cells with aldosterone [5]. Similarly, a portion of total ENaC protein (~30 %) isolated from mouse cortical collecting duct cells ($_{MPK}CCD_{14}$) was detected in low density lipid raft fractions together with the lipid raft marker protein caveolin-1. Hormonal stimulation of ENaC by either forskolin or aldosterone did not alter the lipid raft distribution of ENaC in these cells. Treatment with MβCD reduced ENaC surface expression without affecting the acute stimulatory response to forskolin. Therefore, it was concluded that lipid raft association may be involved in the constitutive apical delivery of ENaC [6]. In A6 epithelial cells cholesterol depletion of the apical membrane had no detectable effect on ENaC surface expression but was found to reduce channel open probability and the stimulatory effects of hypotonicity, adenosine and oxytocin on ENaC-mediated short circuit current [7]. In another study cholesterol depletion of the apical membrane of A6 cells had no apparent effect on the basal Na^+ transport rate but partially inhibited the stimulatory responses to both insulin and ADH [8]. A recent study reports that the lipid raft protein caveolin-1 interacts with ENaC and downregulates channel activity and membrane surface expression [32]. The findings discussed above suggest that cholesterol is a functionally important component of the lipid environment of ENaC. However, at present it is still a matter of debate whether the channel is functionally associated with lipid rafts [33, 34].

The aim of the present study was to investigate the association of ENaC with lipid rafts in the *Xenopus laevis* oocyte expression system using a buoyant density assay, and to study the effect of cholesterol depletion on ENaC

function and its regulation using electrophysiological measurements. Since ENaC regulation by SGK1 is thought to require a complex assembly of regulatory proteins possibly involving lipid rafts, we hypothesized that ENaC activation by SGK1 may be compromised by cholesterol removal.

Materials and Methods

Molecular biology

The full length cDNAs encoding the three subunits of wild-type (wt) rat α-, β- and γENaC [35] were subcloned in the pcDNA3.1 vector (Invitrogen, Karlsruhe, Germany). For detection of the rat αENaC subunit the hemagglutinin (HA) epitope was inserted according to the FLAG epitope placement in the rat sequence [36] and subcloned in pcDNA3.1 vector.

Antibodies

Subunit specific antibodies against β- and γENaC were obtained by immunizing rabbits (Pineda Antibody Service, Berlin, Germany) with keyhole limpet hemocyanin-coupled synthetic peptides corresponding to amino acids within the mouse βENaC sequence (aa 617-638: C-NYD SLR LQP LDT MES DSE VEA I) or within the mouse γENaC sequence (aa 629-650: C-NTL RLD SAF SSQ LTD TQL TNE F) in analogy to previously published sequences of rat ENaC [37]. The sequences of mouse and rat ENaC are highly homologous in this region. Subunit specificity was checked by Western blotting of membrane-enriched fractions of oocytes expressing a single rat ENaC subunit (α, β, or γ) or all three subunits together. Specific binding of the βENaC antibody was further characterized by immunofluorescence staining of rat renal tissue (data not shown). The rat monoclonal antibody against the HA epitope in the α-subunit was obtained from Roche Diagnostics (Mannheim, Germany) and used in a concentration of 1:1000. The polyclonal rabbit affinity isolated antigen specific anti-β-actin antibody (Sigma Aldrich, Taufkirchen, Germany) was used in a dilution of 1:5000. A mouse monoclonal anti-clathrin antibody was obtained from BD Biosciences (Heidelberg, Germany) and used in a concentration of 1:1000. The horseradish peroxidase coupled goat anti-rabbit secondary antibody was obtained from Santa Cruz Biotech (Heidelberg, Germany). A horseradish peroxidase coupled sheep anti-mouse secondary antibody was obtained from Sigma. Both secondary antibodies were used in a dilution 1:10,000. GM-1 was detected with Choleratoxin subunit B conjugated to horseradish peroxidase (Sigma), diluted 1:10,000.

Isolation of oocytes, injection of cRNA, and two-electrode voltage-clamp

Defolliculated stage V-VI oocytes were obtained from ovarian lobes of adult female *Xenopus laevis* in accordance with the principles of German legislation, with approval by the animal welfare officer for the University of Erlangen-Nürnberg, and under the governance of the state veterinary health inspectorate. Animals were anesthetized in 0.2% MS222 (Sigma). Isolation and injection of *Xenopus laevis* oocytes and two-electrode voltage-clamp experiments were performed essentially as described previously [38-41]. Oocytes were injected with cRNA using 0.1, 0.2 or 0.5 ng of cRNA for each subunit per oocyte. To prevent Na^+ overloading, injected oocytes were kept in 'low sodium' modified Barth's saline (low Na^+ MBS) containing in mM: 1 NaCl, 40 KCl, 60 N-methyl-D-glutamine (NMDG)-Cl, 0.3 $Ca(NO_3)_2$, 0.4 $CaCl_2$, 0.8 $MgSO_4$, 10 HEPES, adjusted to pH 7.4 with HCl, supplemented with 100 U ml^{-1} sodium penicillin and 100 µg ml^{-1} streptomycin sulphate. Unless stated otherwise, oocytes were studied 2 days after injection with cRNA. The amiloride-sensitive current (ΔI_{ami}) at a holding potential of -60 mV was determined by subtracting the corresponding value measured in the presence of amiloride (2 µM) from that measured in the absence of amiloride in NaCl solution (in mM: 95 NaCl, 2 KCl, 1 $CaCl_2$, 1 $MgCl_2$, 10 HEPES, adjusted to pH 7.4 with Tris).

Outside-out patch clamp recordings

Recordings in outside-out patches were essentially performed as described previously [31, 42]. Recombinant constitutively active SGK1 (Δ1-60 S422D) was purchased from Biomol GmbH (Hamburg, Germany). Patch pipettes were pulled from borosilicate glass capillaries and had a tip diameter of about 1 µm after fire polishing for single channel recordings (micro-pipettes) and about 5 µm for macroscopic current recordings (macro-pipettes). Pipettes were filled with K-gluconate pipette solution (in mM: 90 K-gluconate, 5 NaCl, 2 Mg-ATP, 2 EGTA, and 10 HEPES, adjusted to pH 7.28 with Tris). Seals were routinely formed in a low sodium NMDG-Cl bath solution (in mM: 95 NMDG-Cl, 1 NaCl, 4 KCl, 1 $MgCl_2$, 1 $CaCl_2$, 10 HEPES adjusted to pH 7.4 with Tris). In this bath solution the pipette resistance averaged about 11 MΩ for micro-pipettes and about 3 MΩ for macro-pipettes. In NaCl bath solution, the NMDG-Cl was replaced by 95 mM NaCl. Outside-out patches were routinely held at a holding pipette potential of -70 mV, which was close to the calculated reversal potential of Cl^- (E_{Cl} = -77.2) and K^+ (E_K = -79.4) under our experimental conditions with experiments performed at room temperature (~23 ºC). Single channel current data were initially filtered at 500 Hz and sampled at 2 kHz. In multi channel patches current traces were re-filtered at 70 Hz to resolve the single channel current amplitude (*i*). Channel activity was derived from binned current amplitude histograms as the product NP_O, where *N* is the number of channels and P_O is open probability [31]. The maximal number of apparent channels (N_{app}) was determined by visual inspection of the traces. To analyze channel gating in patches with multiple channels we calculated the number of channel transitions per second per N_{app} (Transitions x s^{-1} x N_{app}^{-1}) using the program 'Patch for Windows' written by Dr. Bernd Letz (HEKA Elektronik, Lambrecht/Pfalz, Germany). The current level at which all channels are closed was determined in the presence of 2 µM amiloride. The macroscopic current traces were sampled at 400 Hz and filtered at 100 Hz. Data are presented as mean values ± SEM; *n* indicates the number of individual oocytes; N indicates the number of different batches of oocytes used. Appropriate versions of Student's *t* test were used. *p* values less than 0.05 were required to reject the null

hypothesis. *, **, and *** represent p values smaller than 0.05, 0.01, and 0.001, respectively.

Cholesterol depletion of the plasma membrane of intact oocytes by MβCD

For electrophysiological experiments intact oocytes were preincubated in 20 mM MβCD (Sigma) or mannitol in low Na^+ MBS solution for 3 hours at 19 °C. Filipin staining of intact living oocytes was used to confirm that the pretreatment with MβCD efficiently depletes cholesterol from the plasma membrane. For this purpose oocytes were incubated for 1 h with 0.05 mg/ml filipin (Sigma) in low Na^+ MBS at room temperature, washed 3 times with low Na^+ MBS and incubated in low Na^+ MBS containing either 20 mM MβCD or 20 mM mannitol. During the incubation period in MβCD or mannitol, oocytes were regularly inspected with a Zeiss inverted fluorescent microscope (Axiovert 200 M, Zeiss, Göttingen, Germany) with the apotome technique using excitation filter BP 350-410 nm for filipin and a 40 x water immersed Acroplan objective. Images of regions of the cell membrane of intact oocytes were taken at different time points using a constant exposure time and were analyzed with the help of the Axiovision software (Zeiss).

Preparation of non-detergent membrane-enriched fractions

50 oocytes, each injected with cRNAs for HA- tagged αENaC, wild-type rat β- and γENaC (0.5 ng per subunit), were lysed in 500 µl non-detergent lysis buffer [43], containing 250 mM sucrose, 1 mM EDTA, 20 mM Tris, pH 7.8, and protease inhibitors (Roche Diagnostics, Mannheim, Germany) by aspiration (5 times) through a 27-gauge needle and sonication (3 times 5 sec at 4 °C). MβCD or mannitol from 100 mM stock solutions were added to the oocyte homogenates to give a final concentration of 20 mM and incubated for 30 min at room temperature. Nuclei and cell debris were removed from the homogenates by centrifugation at 1000 g. The postnuclear supernatants were centrifuged at 21,100 g to obtain membrane-enriched fractions in the pellet and cytosolic proteins in the supernatant. Total membrane pellets were resuspended in 330 µl of non-detergent lysis buffer including protease inhibitors. Functional ENaC expression was confirmed in oocytes from the same batch by measuring the amiloride-sensitive current 48 h after cRNA injection (data not shown).

Biotinylation of ENaC subunits on the cell surface of oocytes

To separate cell surface membrane proteins from intracellular membrane proteins, cell surface proteins were labelled with biotin as previously described [42, 44] using 50 oocytes per experimental condition. All biotinylation steps were performed at 4 °C. In brief, oocytes were chilled to 4 °C by transferring oocytes 3 times into ice-cold low Na^+ MBS. Oocytes were biotinylated in biotinylation buffer containing 10 mM triethanolamine, 150 mM NaCl, 2 mM $CaCl_2$, and 1 mg/ml EZ-link sulfo-NHS-SS-Biotin (Pierce, Rockford, Illinois, USA), pH 9.5 for 15 min with gentle agitation. The reaction was stopped by washing the oocytes 2 times in a quenching buffer containing 192 mM glycine, 25 mM Tris, pH 7.5 and by incubation in the quenching buffer with gentle agitation for 5 min. Subsequently, oocytes were lysed by aspiration (5 times) through a 27-gauge needle in 500 µl non-detergent lysis buffer (see above) including protease inhibitors. Total protein amount was determined by a BCA-Assay (Pierce). Biotinylated proteins were captured by 50 µl immunopure immobilized Neutravidin agarose beads (Pierce) previously washed with lysis buffer. After overnight incubation at 4 °C on a rotating wheel, the beads were centrifuged for 3 min at 10,000 g and supernatants were collected separately for the detection of non-biotinylated intracellular membrane proteins. Beads were washed three times with lysis buffer and finally resolved in 50 µl twofold reducing SDS-PAGE sample buffer (Rotiload 1, Roth, Karlsruhe, Germany). Proteins were eluted by boiling and the whole protein sample was used for Western blot analysis. Aliquots of 25 µg of intracellular membrane proteins were loaded on the same gel together with the corresponding eluates of biotinylated cell surface membrane proteins.

Separation of raft and non-raft membranes by discontinuous sucrose gradient centrifugation

The membrane-enriched fraction was resuspended in 330 µl of non-detergent buffer and mixed with 348 µl of an 85 % sucrose solution (w/v) in 1 mM EDTA/20 mM Tris, pH 7.8 to reach a final concentration of 45 % sucrose. The sample was then overlaid with 2.0 ml 35 % sucrose solution (w/v) and 1.3 ml 5 % sucrose solution (w/v). Sucrose gradients were centrifuged at 100,000 g for 18 h at 4 °C in a SW 60 rotor (Beckman-Coulter, Krefeld, Germany). 12 fractions of 330 µl each were collected from the top to the bottom. In the same way sucrose gradient experiments were performed using samples enriched with cytosolic proteins (see above).

Western blotting

All samples of biotinylated and non-biotinylated proteins were heated for 5 min at 95 °C before loading on SDS-gels. Biotinylated proteins and aliquots of non-biotinylated total proteins were separated by 10 % and 12 % SDS-PAGE respectively, transferred to PVDF membranes by semi-dry electroblotting and probed with the indicated antibodies. Chemiluminescent signals were detected using ECL plus (Amersham, GE Healthcare, UK).

Results

ENaC expressed in Xenopus laevis oocytes is present in putative lipid raft fractions

The initial aim of our study was to confirm in the *Xenopus laevis* oocyte expression system that ENaC is associated with putative lipid raft fractions of low density in a floatation assay. We used a similar approach as previously described to demonstrate the association of ENaC with lipid rafts in cultured renal epithelial cells [5, 6]. After non-detergent cell lysis membranes of different buoyant density were prepared from oocytes heterologously

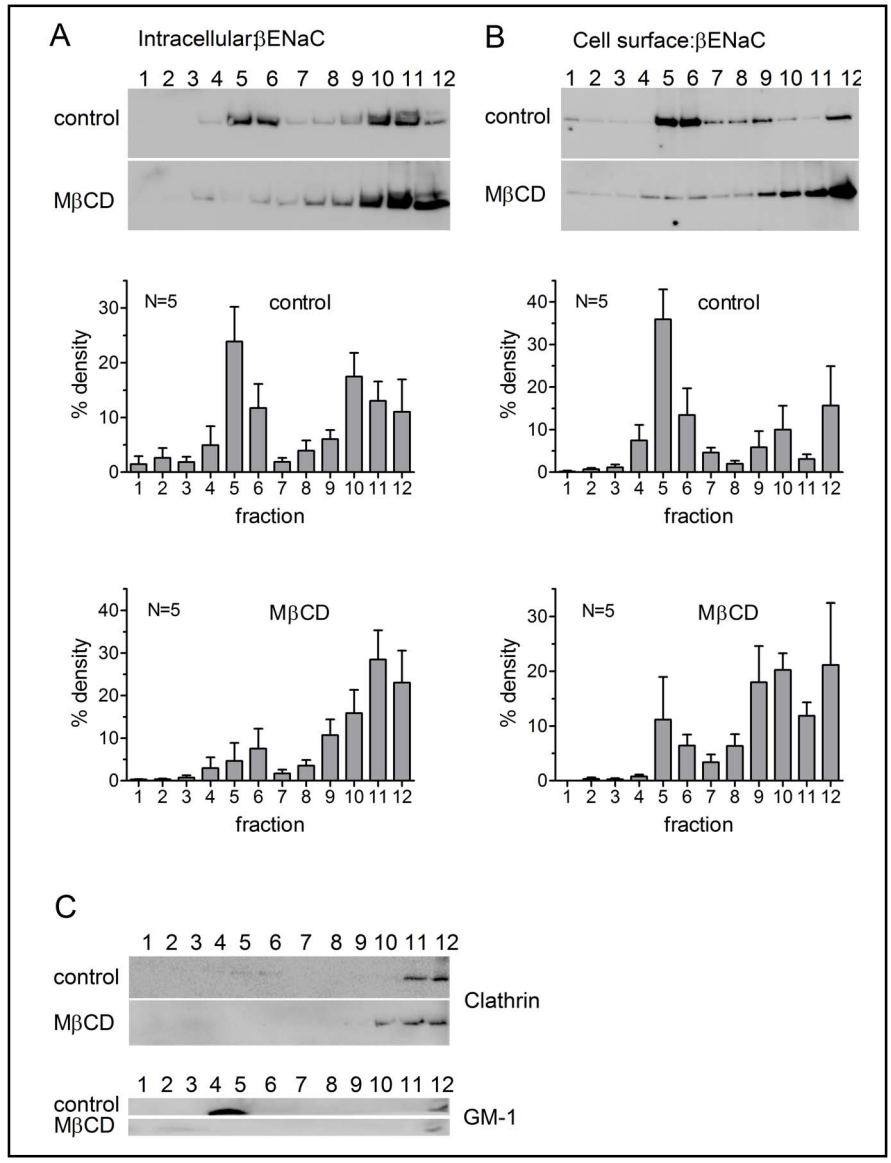

Fig. 1. ENaC is present in lipid raft fractions. Homogenates of biotinylated rat αβγENaC expressing oocytes were incubated with 20 mM MβCD or mannitol (control) for 30 min at room temperature. Membrane-enriched fractions were loaded on discontinuous sucrose gradients. To separate cell surface membrane proteins from intracellular membrane proteins, cell surface proteins were biotinylated. ENaC distribution was studied by Western blot detection of the β-subunit. A,B. Representative blots and densitometric summary of five similar experiments using different batches of oocytes demonstrating non-biotinylated intracellular (A) and biotinylated surface (B) βENaC expression after mannitol (control) or MβCD treatment. C. Representative Western blots demonstrating the expression of the lipid raft marker GM-1 and the non-raft marker clathrin. Fractions were taken from the top (1, lowest density) to the bottom (12, highest density) of the sucrose gradients. N indicates number of different batches of oocytes used.

expressing rat αβγENaC. Distribution of ENaC in sucrose density gradient fractions was analyzed by Western blotting using biotinylated cell surface proteins and non-biotinylated intracellular proteins. For reliable ENaC detection we used an antibody against the β-subunit of the channel because unlike α- and γENaC the β-subunit is not proteolytically processed [29]. As shown in the control blots in figure 1A and 1B a substantial portion of the intracellular and the biotinylated cell surface pool of ENaC could be detected in putative lipid raft fractions of low density. The lipid raft marker GM-1 was used to confirm that the low density fractions are likely to correspond to lipid raft fractions (figure 1C). Moreover, we demonstrated that clathrin was not detectable in the putative lipid raft fractions but was present in the higher density fractions as expected for a non-raft protein (figure 1C). Importantly, pretreatment of cell lysates with 20 mM MβCD shifted ENaC from the putative lipid raft fractions of low density to fractions of higher density in both the intracellular and the cell surface pool of ENaC (figure 1A and 1B). As expected the signal for GM-1 in the low density fractions also disappeared when oocyte lysates were treated with MβCD (figure 1C). Taken together our results indicate that ENaC is associated, at least in part, with cholesterol-enriched lipid raft membrane domains in *Xenopus laevis* oocytes and that *in vitro* cholesterol depletion can disrupt this association.

MβCD effectively removes cholesterol from the plasma membrane of living oocytes

To establish that MβCD is an appropriate tool to remove cholesterol from the oocyte plasma membrane of

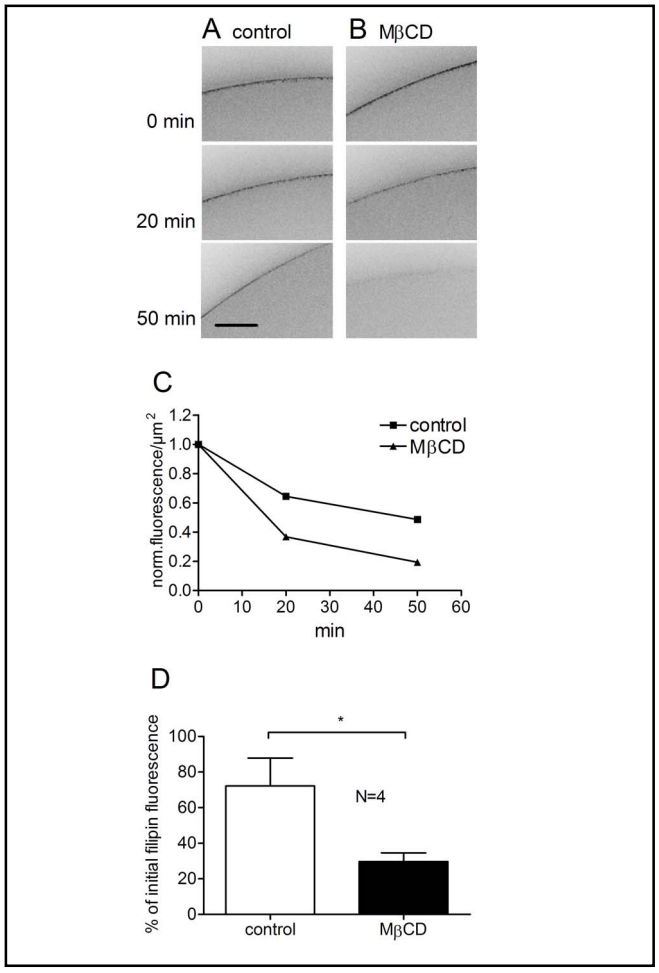

Fig. 2. MβCD effectively removes cholesterol from the plasma membrane of living oocytes. A,B. Oocytes were incubated with filipin in low Na^+ MBS for 1 h and subsequently transferred to a low Na^+ MBS containing either 20 mM mannitol (control) (A) or 20 mM MβCD (B). The fluorescence signal of filipin bound to plasma membrane cholesterol was monitored in living intact oocytes. Images of representative membranes were taken at different time points (0, 20, and 50 min) after transfer to the MβCD or control solution using a constant exposure time. Scale bar indicates 50 μm. C. Time course of the fluorescence decline in control and MβCD treated oocytes using the data shown in A and B. D. Average relative decline of the fluorescence signal after a ~30 minute incubation in control or MβCD determined in four similar experiments as shown in A-C. N indicates number of different batches of oocytes used, * $p<0.05$.

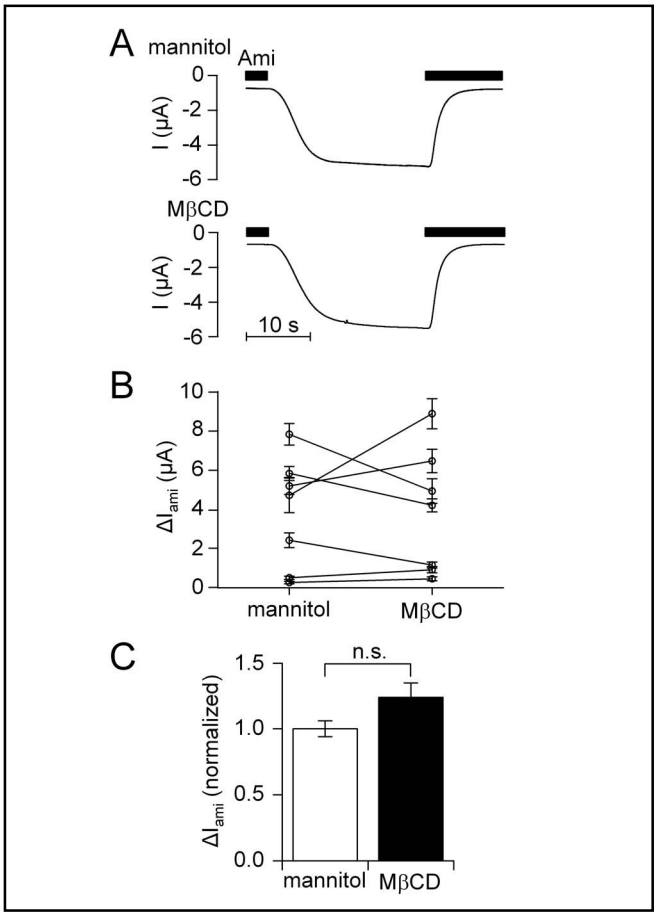

Fig. 3. Cholesterol depletion has no consistent effect on ENaC-mediated whole-cell currents. A. Representative whole-cell current traces of two αβγENaC expressing oocytes after 20 mM mannitol (control, upper trace) or 20 mM MβCD (lower trace) treatment for 3 h. Amiloride (2 μM) was present in the bath as indicated by the black bars to specifically inhibit ENaC and to determine the amiloride-sensitive whole-cell current (ΔI_{ami}). B. Average ΔI_{ami} data obtained in independent experimental series using seven different batches of oocytes. Symbols and error bars indicate mean and SEM, respectively. Lines connect the average ΔI_{ami} values measured in oocytes from the same batch. C. Normalized summary of the experiments shown in B. Individual ΔI_{ami} values were normalized to the mean value of the corresponding mannitol treated control group and pooled (control: n=82; MβCD: n=81). n.s. not significant.

living oocytes, we used filipin, a fluorescent antibiotic that binds to cholesterol in the plasma membrane [45]. As shown in figure 2, fluorescent micrographs of plasma membrane regions of individual oocytes were taken at different time points using a constant exposure time. A fluorescence signal representing filipin bound to plasma membrane cholesterol was detectable in filipin treated but not in non-treated native oocytes (data not shown). In control oocytes, the filipin fluorescence signal decreased spontaneously over time (figure 2A). However, the decline of the filipin fluorescence signal was much more pronounced in oocytes exposed to 20 mM MβCD (figure 2B). Figure 2 C illustrates the time course of the decline of the filipin fluorescence signal in mannitol and MβCD treated oocytes using the data from the representative experiments shown in figure 2A and 2B.

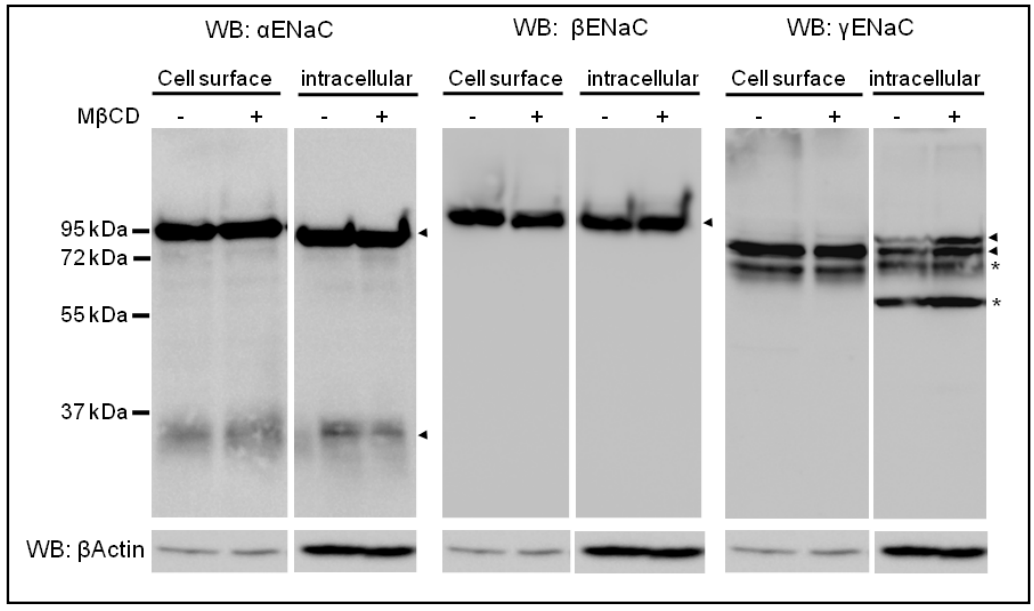

Fig. 4. MβCD does not alter cell surface expression and cleavage of ENaC. $\alpha_{HA}\beta\gamma$ENaC expressing oocytes were biotinylated after incubation with 20 mM MβCD or mannitol (control) for 3 h. Membrane-enriched fractions were used, and cell surface proteins were separated from intracellular proteins with Neutravidin beads. Using Western blot analysis, the αENaC subunit was detected with an antibody against the HA-epitope. β- and γENaC subunits were detected with mouse ENaC subunit specific antibodies. Arrow heads indicate the expected bands characteristic for the full length or known cleaved forms of the subunits. * indicate unspecific bands. The blots were reprobed with an antibody against the cytoskeletal protein β-actin to demonstrate the efficient separation between cell surface and intracellular proteins and to demonstrate that similar amounts of protein were loaded per lane.

Results from four similar experiments are summarized in figure 2D. The effect of MβCD could be stopped by changing the incubation solution from MβCD to control solution. In this case, no further decrease of fluorescence was observed (data not shown). Taken together these results demonstrate that MβCD effectively depletes cholesterol from the plasma membrane of intact oocytes with a significant effect after about 50 min exposure. Based on these results we decided to use a preincubation time of three hours to achieve a maximal effect of MβCD to test the effect of plasma membrane cholesterol removal on ENaC activity.

Cholesterol depletion has no consistent effect on whole-cell currents in oocytes heterologously expressing ENaC

Oocytes heterologously expressing rat αβγENaC were pretreated for three hours with 20 mM MβCD or with 20 mM mannitol as osmotic control. Subsequently, the amiloride-sensitive whole-cell ENaC current (ΔI_{ami}) was measured by two-electrode voltage-clamp at a holding potential of -60 mV. Figure 3A shows typical whole-cell current traces obtained in an oocyte exposed to MβCD and in a control oocyte exposed to mannitol. The experiments were started in the presence of amiloride (2 μM) in the bath solution known to specifically inhibit ENaC. Washout of amiloride resulted in the appearance of an inward current component reflecting ENaC mediated sodium inward current. Reapplication of amiloride resulted in a return of the current to its baseline level. Qualitatively, the whole-cell current traces of MβCD treated oocytes looked similar to those recorded in control oocytes. In figure 3B results obtained in seven different batches of oocytes are shown for each individual batch. From these results it can be seen that the effect of MβCD on ΔI_{ami} varied slightly from batch to batch. Indeed, pretreatment with MβCD appeared to increase average ΔI_{ami} in four batches of oocytes while it decreased ΔI_{ami} in the remaining three batches (figure 3B). Normalization of the data to summarize results from all seven batches did not reveal a significant effect of MβCD on ΔI_{ami} (figure 3C).

MβCD does not alter cell surface expression and cleavage of ENaC

Our whole-cell current measurements demonstrated that pretreating oocytes for three hours with MβCD had no consistent effect on ENaC baseline currents, which is in good agreement with the variable effect of MβCD on ENaC function previously reported in other systems [7, 8]. The lack of a significant functional effect of MβCD on ENaC baseline whole-cell currents also fits to our Western blot data shown in figure 4. These results indicate that pretreating intact oocytes with 20 mM MβCD for three hours does not alter the surface expression of the three ENaC subunits and has no apparent effect on the cleavage pattern of the α- and γ-subunits. Proteo-

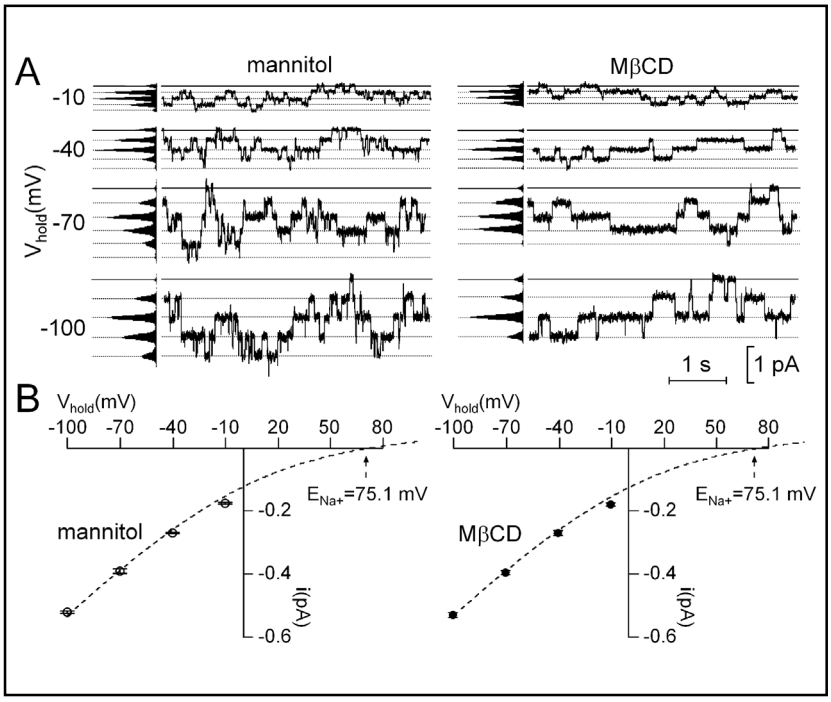

Fig. 5. MβCD does not alter the single channel conductance of ENaC. A. Representative single channel current traces at different holding potentials (V_{hold}) from outside-out patches of αβγENaC expressing oocytes. The current level at which all channels are closed was determined in the presence of amiloride and is indicated by a solid line. The different channel open levels are indicated by horizontal dotted lines. Binned current amplitude histograms (shown to the left of the traces) were used to determine the single channel current amplitude (i) at each holding potential. On the left hand side the traces were recorded in a patch from a control oocyte (20 mM mannitol; 3h) and on the right hand side from an oocyte treated with MβCD (20 mM; 3h). B. Average single channel I/V plots from control (open circles; n=9; N=3) and MβCD treated oocytes (filled circles; n=10; N=3). Vertical bars represent SEM values. The dashed line represents a GHK fit of the data for a Na^+ selective channel with a predicted Na^+ equilibrium potential (E_{Na}) of 75.1 mV.

lytic cleavage of the latter two subunits is known to be involved in ENaC processing and activation [29, 46]. The bands shown in figure 4 nicely correspond to previously reported full length and cleaved forms of the three ENaC subunits [29, 42, 47, 48]. Importantly, the ENaC fragments detected at the cell surface were not different in the MβCD treated oocytes compared to those in control oocytes. For the α-subunit we detected the expected ~30 kDa fragment in addition to the full length form of ~95 kDa which results from endogenous cleavage by furin directly after the inserted HA-tag in this construct. For the γ-subunit the 76 kDa cleaved fragment was the most prominent fragment at the cell surface which is consistent with previous reports from other laboratories and our own findings [29, 42, 47, 48]. In the intracellular protein fraction we also detected a ~87 kDa band most likely corresponding to full length γENaC. The additional ~68 kDa and ~60 kDa bands detected by our γENaC antibody are most likely unspecific bands and do not represent γENaC cleavage products since they are also present in non-injected oocytes and in oocytes expressing αENaC or βENaC alone (data not shown). Interestingly, the 60 kDa unspecific band was detected in the intracellular protein fraction of both, control and MβCD treated oocytes, but was absent at the cell surface. This finding confirms that the biotinylation approach effectively distinguishes between the intracellular and cell surface pool of proteins. This is further supported by the intense signal for the cytoskeletal protein β-actin detected in the intracellular protein pool whereas only a faint β-actin band was detectable in the cell surface pool. Thus, contamination of the cell surface pool with intracellular proteins is minimal. In conclusion these data indicate that in intact oocytes cholesterol removal by MβCD has little effect on ENaC surface expression and on channel cleavage at the cell surface, consistent with the absence of a significant effect of MβCD on ENaC whole-cell currents.

Effect of cholesterol removal on single channel properties of ENaC in outside-out patches

To investigate a potential effect of cholesterol removal by MβCD on single channel properties of ENaC, we performed outside-out patch clamp experiments as previously described [31, 42]. Outside-out patches were obtained from oocytes expressing αβγENaC. Figure 5A shows typical single channel current traces recorded at different holding potentials in an outside-out patch from an oocyte pretreated for three hours with 20 mM MβCD or with 20 mM mannitol as osmotic control. Corresponding I/V plots are shown in figure 5B. These data indicate that pretreatment with MβCD does not alter the sodium selectivity of the channel and does not change its single channel conductance. The latter averaged 5.59 ± 0.09 pS (n=9, N=3) and 5.63 ± 0.10 pS (n=10, N=4) in mannitol and MβCD pretreated oocytes, respectively. This single channel conductance is typical for ENaC and in good agreement with previously reported values [1, 3, 31, 35, 42]. Moreover, we confirmed that ENaC in outside-out

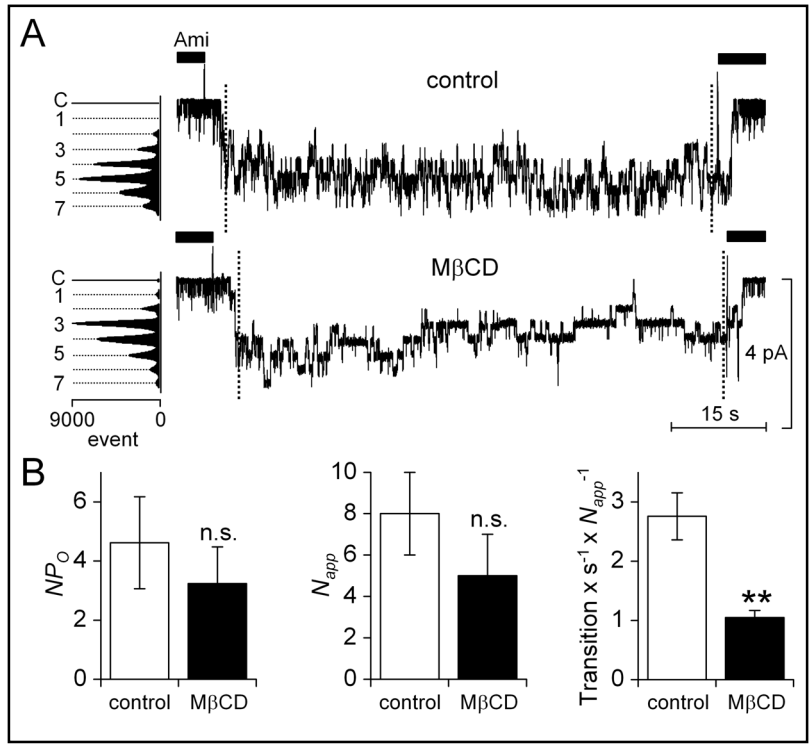

Fig. 6. MβCD slightly changes the single channel kinetics of ENaC. A. Representative single channel current traces at a holding potential (V_{hold}) of -70 mV from outside-out patches of αβγENaC expressing oocytes pretreated for 3h with mannitol (control, upper trace) or MβCD (lower trace). The binned current amplitude histograms displayed to the left of the traces were obtained from the recording intervals delineated by the vertical dotted lines and were used to calculate channel activity (NP_O). The maximal number of apparent channels (N_{app}) was determined by visual inspection of the traces. B. Averaged values of NP_O, N_{app}, and the number of channel transitions per second per N_{app} (Transition x s^{-1} x N_{app}^{-1}) evaluated from several recordings as shown in A (control: n=9, N=3; MβCD: n=10, N=3). n.s. not significant, ** p<0.01.

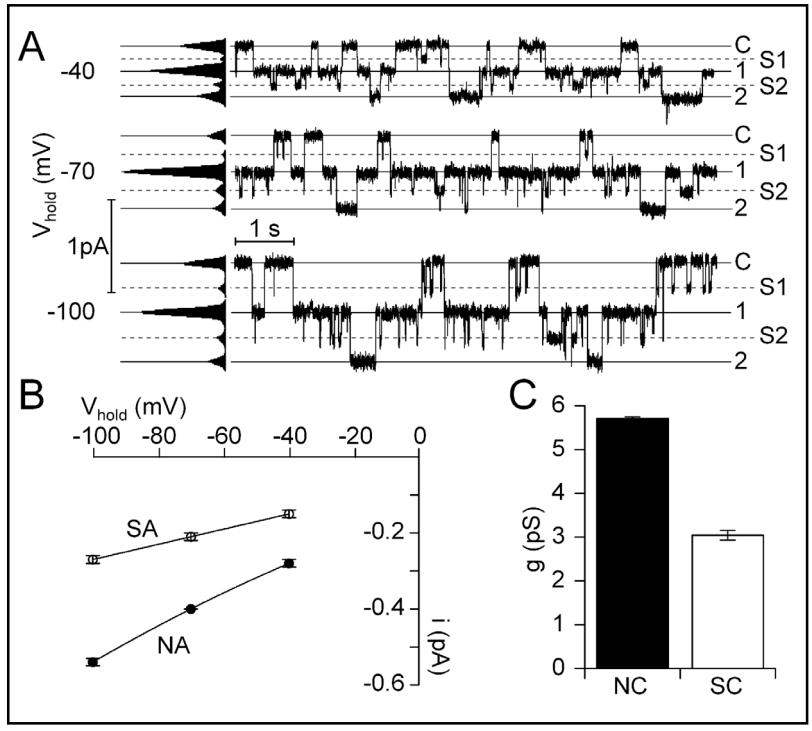

Fig. 7. Subconductance states of ENaC occur in outside-out patches from MβCD-treated oocytes. A. Representative single channel current traces at different holding potentials (V_{hold}) from an outside-out patch of an αβγENaC expressing MβCD pretreated (3h) oocyte. The current level at which all channels are closed (C) was determined in the presence of amiloride. The solid lines represent the normal single channel current levels (1, 2). Dashed lines show current levels of single channel events with reduced current amplitude ("Sublevels"; S1, S2). Binned current amplitude histograms are shown to the left of the traces. B. Average *I/V* plots of single channel events with "subnormal amplitudes" (SA; open circles) and with "normal amplitudes" (NA; filled circles) as detected in four different outside-out patches as shown in A. C. Average single channel slope conductance (g) derived from the single channel current amplitudes (same data as shown in B) measured at a holding potential of -100 mV and -70 mV are shown for the "subconductance" (SC; open column) and the "normal conductance" state (NC; filled column).

patches from mannitol and MβCD pretreated oocytes could be inhibited by the addition of 2 μM amiloride to the bath solution. This is illustrated in the representative traces shown in figure 6A. Interestingly, the gating kinetics of the channels in patches from MβCD pretreated oocytes appeared to be slightly slower than those of the channels in control patches (figure 5A and 6A). However, the estimated values for overall channel activity (NP_O) and apparent number of channels per patch (N_{app}) were not significantly different in outside-out patches from MβCD pretreated oocytes compared to those in patches from mannitol treated control oocytes (figure 6B). This is in good agreement with our finding that the whole-cell ENaC currents were similar in mannitol and MβCD pretreated

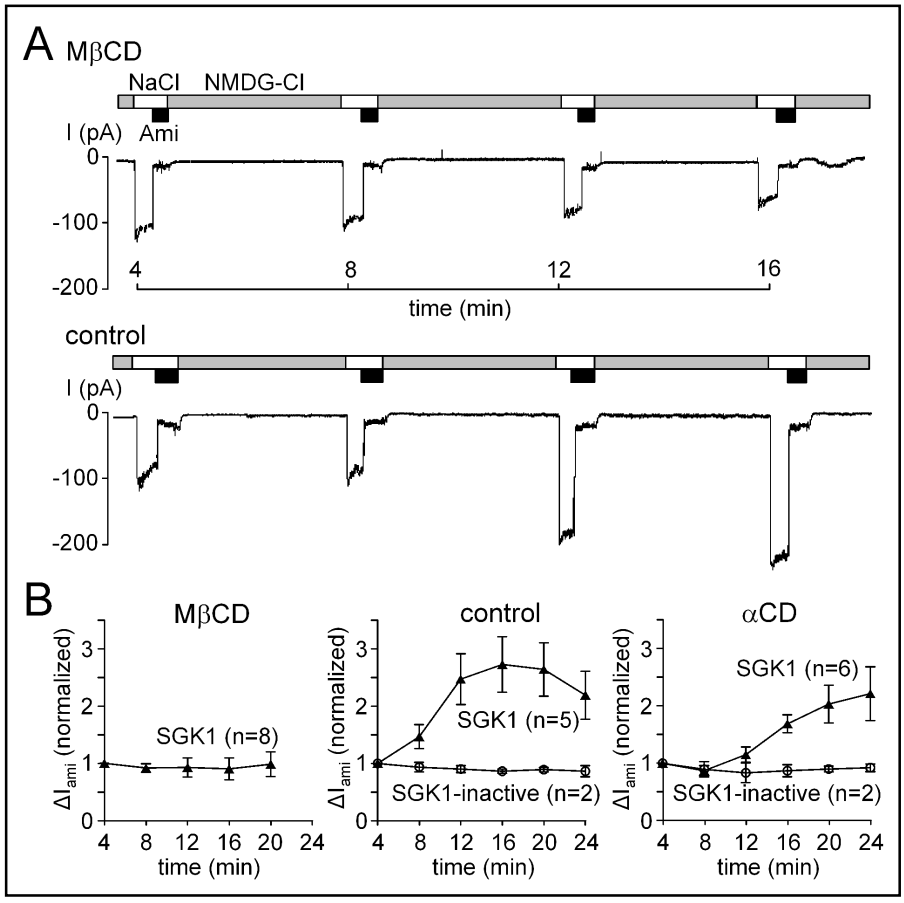

Fig. 8. MβCD abolishes the stimulatory effect of SGK1 on ENaC currents. A. Representative current (I) traces from outside-out macropatches of MβCD (upper trace) and mannitol (lower trace) pretreated αβγENaC expressing oocytes recorded at a holding potential (V_{hold}) of -70 mV. To prevent channel rundown the patches were superfused with a low Na^+ (1 mM) containing NMDG-Cl solution. For the detection of the amiloride-sensitive component NMDG-Cl was replaced by NaCl (95 mM) and amiloride (2 μM) was applied as indicated by the white and black bars, respectively. Constitutive active recombinant SGK1 (80 U/ml) was present in the pipette solution to activate ENaC. B. Normalized summary of data from similar experiments of MβCD and mannitol (control) pretreated oocytes as shown in A and, as additional control, α-cyclodextrin (αCD) pretreated oocytes. For both control groups heat-inactivated SGK1 was used as a negative control (SGK1-inactive). *n* indicates number of different patches.

oocytes. To substantiate our impression that MβCD affects channel gating, we counted the overall number of channel transitions per time in multi channel recordings like those shown in figure 6A. Interestingly, the average number of observed transitions per second and per N_{app} was significantly reduced in outside-out patches from MβCD pretreated oocytes. This suggests that cholesterol removal by MβCD slightly reduces the frequency of gating events. If this resulted in a roughly equal increase of both, mean channel open and mean channel closed times, the altered gating kinetics would have little effect on the average channel open probability. This would explain the absence of a significant effect of MβCD on ENaC whole-cell currents despite altered channel kinetics. Unfortunately, we were unable to obtain patches with only one active channel in the patch which would be necessary for a more detailed analysis of the apparent effect of MβCD on channel gating.

In addition to slightly altered channel kinetics, we observed channel conductance sublevels in four out of ten outside-out patches from MβCD pretreated cells but not in outside-out patches from control cells (n=9). The smaller single channel transitions were abolished in the presence of amiloride (data not shown), which confirms that there are conductance sublevels of ENaC and cannot be attributed to other non-related channels in the patch. Typical current traces containing full sized single channel current events and additional events with a reduced current amplitude are shown in figure 7A with the corresponding *I/V* plots shown in figure 7B. In four similar recordings the single channel conductance calculated for the reduced and the full channel openings averaged 3.04 ± 0.11 pS and 5.71 ± 0.04 pS (*n*=4, N=2), respectively. Our observation that MβCD pretreatment may cause the appearance of ENaC conductance sublevels in at least some of the patches is in good agreement with a recent report that ENaC subconductance events were observed in A6 cells after treatment with 50 mM MβCD [49]. Collectively, our findings indicate that cholesterol removal has significant effects on the single channel properties of ENaC.

MβCD abolishes the stimulatory effect of recombinant SGK1 on ENaC in outside-out patches

We previously demonstrated that recombinant SGK1 included in the pipette solution can activate ENaC in outside-out patches and that this stimulatory effect critically

depends on a specific serine residue in the channel's α-subunit [31]. To analyze whether the stimulatory effect of SGK1 depends on the lipid microenvironment of the channel and can be affected by cholesterol depletion by MβCD, we performed recordings in outside-out macropatches from *Xenopus laevis* oocytes expressing rat αβγENaC with recombinant SGK1 in the pipette solution. ENaC activity was monitored in these patches by repeatedly measuring the amiloride-sensitive current (ΔI_{ami}) as illustrated in the two representative current traces shown in figure 8A. The top current trace was obtained from an oocyte pretreated with 20 mM MβCD for three hours. In this patch ΔI_{ami} was not stimulated by SGK1 and even showed a small degree of rundown over time. In contrast, in the patch obtained from a matched control oocyte (bottom trace), we observed the expected stimulatory effect of SGK1 on ΔI_{ami} as previously described [31]. Data from similar experiments are summarized in figure 8B and confirm the absence of a stimulatory effect of SGK1 in outside-out patches from oocytes pretreated with MβCD (n=8). Similarly, no stimulation of ΔI_{ami} was observed in outside-out patches from control oocytes with heat-inactivated SGK1 in the pipette solution (n=2). In contrast, including SGK1 in the pipette solution had a robust stimulatory effect in outside-out patches from control oocytes (n=5). As an additional control we used α-cyclodextrin (αCD), a reagent with an MβCD-like chemical structure but unable to extract cholesterol from the plasma membrane. Pretreating oocytes with αCD failed to abolish the stimulatory effect of SGK1 (n=6), which indicates that the effect of MβCD is specific. Taken together these results indicate that cholesterol removal from the plasma membrane prevents ENaC stimulation by cytosolic SGK1.

Discussion

In this study we made three key observations: First, we demonstrated that rat ENaC heterologously expressed in *Xenopus laevis* oocytes is associated with putative lipid raft fractions in a floatation assay. Secondly, we demonstrated that removal of plasma membrane cholesterol by MβCD had no consistent effect on baseline ENaC whole-cell currents but had subtle effects on channel kinetics and was associated with the occasional appearance of conductance sublevels in single channel recordings. Finally, the most prominent finding of our study is that cholesterol removal from the plasma membrane abolishes the stimulatory effect of SGK1 on ENaC in outside-out patches. Taken together, our results demonstrate that the lipid environment of the channel and the cholesterol content of the plasma membrane is an important determinant of ENaC function and regulation.

Our results suggest that at the cell surface and in intracellular compartments ENaC is present in both, lipid raft and non-raft fractions. This is consistent with previous findings [5] and may indicate that the association of ENaC with cholesterol-enriched fractions is not constant during the channel's turnover. Indeed, it has previously been reported that ENaC becomes Triton X-100 insoluble along the biosynthetic pathway when subunits assemble in the plasma membrane [34, 50]. To confirm ENaC association with cholesterol-enriched membrane microdomains, we treated oocyte homogenates with MβCD to maximize cholesterol depletion from all cellular membranes [51]. Cholesterol depletion of the membrane preparation shifted ENaC out of the putative lipid raft fractions. Taken together these findings support the conclusion of previous studies that ENaC is at least in part associated with cholesterol-rich lipid raft microdomains [5, 6].

Interestingly, treating intact oocytes for three hours with 20 mM MβCD to remove plasma membrane cholesterol had no consistent effect on baseline ENaC whole-cell currents. This is in good agreement with recent findings [7] that membrane cholesterol extraction did not significantly affect the electrophysiological parameters of A6 renal epithelial cells under steady-state conditions. Some studies suggested that a high cholesterol content of the plasma membrane tends to stabilize ENaC function [49]. In contrast, reducing plasma membrane cholesterol was reported to impair ENaC function but with rather variable effects [7, 8, 49, 52]. We also observed somewhat variable effects of cholesterol depletion on ENaC baseline currents in oocytes which may be attributed to an incomplete removal of cholesterol from the plasma membrane in intact cells. This hypothesis is supported by the finding that in intact cells cholesterol depletion of the outer leaflet of the plasma membrane by MβCD may be partially compensated by efficient translocation of cholesterol from the inner to the outer leaflet [52]. This may prevent a complete loss of cholesterol from the outer leaflet of the plasma membrane. Thus, a variable degree of plasma membrane cholesterol removal may be the reason why we did not observe a consistent effect of 20 mM MβCD on baseline ENaC whole-cell currents.

Our single channel recordings from outside-out patches of oocytes pretreated with MβCD suggest that

cholesterol removal has subtle effects on the kinetics of the channel and leads to the occasional appearance of conductance sublevels. The latter finding is consistent with a previous report that subconductance states of ENaC can be observed in A6 cells after cholesterol depletion from the luminal membrane by MβCD (50 mM) [49]. Thus, it is tempting to speculate that a change in the cholesterol content of the plasma membrane may slightly alter the channel's conformation thereby inducing subconductance states and changes in channel kinetics.

To study whether ENaC trafficking to the cell surface is altered by MβCD treatment, we analyzed the expression of ENaC at the cell surface using biotinylation experiments. We found no evidence for a major effect of MβCD on ENaC surface expression. This is in good agreement with previously reported data from A6 renal epithelial cells, in which apical MβCD treatment (10-20 mM for 60 min) did not significantly alter the density of conducting channels at the cell surface as demonstrated by transepithelial capacitance measurements and noise analysis [7]. In contrast, it has been reported that apical exposure of cultured mCCD mouse collecting duct cells to 10 mM MβCD for 60 min reduces ENaC-mediated sodium transport by about 40 % with a concomitant reduction in ENaC surface expression assessed in biotinylation experiments [6]. The reason for this discrepancy with our findings is presently unclear but may be the result of the different experimental systems used. Thus, we cannot rule out the possibility that under certain conditions cholesterol depletion of the plasma membrane may affect ENaC trafficking.

The most prominent finding of our study is the observation that cholesterol removal from the plasma membrane essentially abolishes the stimulatory effect of SGK1 on ENaC in outside-out patches. Our finding that cholesterol depletion prevents ENaC stimulation by SGK1 is in good agreement with the recently reported finding that apical MβCD application hampered ENaC activation by hypotonicity, adenosine, oxytocin, ADH, and insulin [7, 8]. In previous reports it has been shown that the regulation of ENaC involves phosphorylation and dephosphorylation events [53-56]. We have previously demonstrated that SGK1 stimulates amiloride-sensitive currents in outside-out membrane patches of *Xenopus laevis* oocytes expressing ENaC [31]. The stimulatory effect of SGK1 depends on the presence of the S621 serine residue in the SGK-consensus motif in the α-subunit and is likely to be mediated by channel phosphorylation. However, at present it remains an unanswered question whether SGK1 phosphorylates the S621 residue directly or whether downstream kinases and/or phosphatases are involved. Our finding that plasma membrane cholesterol removal abolishes the stimulatory effect of SGK1 indicates that additional regulatory proteins associated with lipid rafts are necessary to mediate the stimulatory effect of SGK1 on ENaC and may be associated with the channel in cholesterol-rich lipid raft microdomains. Currently, several groups report the existence and functional importance of multi-protein complexes where cholesterol is recruited [32, 57, 58]. The specific role for cholesterol in these complexes might be to stabilize the lipid bilayer in this region and to facilitate protein-protein interaction. Findings from related proteins suggest that ENaC may also be associated with regulatory proteins in a multi-protein complex. For example it has been reported that MEC-4 and MEC-10, which belong to the family of degenerin/ENaC Na^+-channels, are associated in such a complex with the cholesterol-recruiting protein MEC-2. Moreover, an interaction with cholesterol seems to be important for the activity of the MEC-4/MEC-10 channel [59, 60] (for review see [57]).

Recently it has been reported that ENaC is regulated by the lipid raft marker protein caveolin-1. Moreover, the coordinated down regulation of ENaC by caveolin-1 and Nedd4-2 suggests a co-localization of these proteins in lipid rafts [32]. Indeed, the ubiquitin-ligase Nedd4 has been found to be present in Triton X-100 resistant membranes [61]. Interestingly, it has been reported that a signalling complex that modulates ENaC surface expression consists of Nedd4-2 and Raf-1 as inhibitory components with SGK1 and the Raf-1 interacting protein glucocorticoid-induced leucine zipper (GILZ1) as stimulatory components [62]. Raf-1 has been reported to be a detergent resistant protein and may be localized in lipid rafts [63]. Moreover, CAP-1, a channel activating protease known to activate ENaC, is a GPI-anchored protein [64] and may distribute to lipid raft microdomains. Thus, a functional association of ENaC with membrane bound proteases within lipid rafts may be relevant for proteolytic ENaC activation. Finally, phospholipids such as phosphatidylinositol-bisphosphates (PIP_2) are reported to regulate ENaC activity *via* direct binding of the β- and γ-subunit (for review see [65]) and are expected to be specifically located in raft-like domains (for review see [66]). Taken together these findings suggest that the lipid environment of ENaC may be important for ENaC's interaction with regulatory proteins, for channel trafficking to the apical membrane, for channel internalisation, or for the regulation of ENaC activity by proteases, phosphatases, and kinases.

We conclude that cholesterol is a critical component of an assembly platform for regulatory proteins required in close proximity of ENaC to mediate the stimulatory effect of SGK1 on the channel.

Acknowledgements

The expert technical assistance of Ralf Rinke, Jessica Ott and Céline Harlay is gratefully acknowledged. We thank Johannes Loffing for his help with the characterization of the antibodies. This study was supported by grants of the Deutsche Forschungsgemeinschaft (SFB423: Kidney injury: Pathogenesis and Regenerative Mechanisms; project A12; C.K.), the Johannes and Frieda Marohn Stiftung (C.K.), an Elitenetwork Bavaria (ENB) fellowship (S.H.), and the BioMedTec International Graduate School (BIGSS) 'Lead Structures of Cell Function' of the ENB (S.H.), and by a travel grant to B.K. from the Fritz Thyssen Foundation.

References

1 Garty H, Palmer LG: Epithelial sodium channels: function, structure, and regulation. Physiol Rev 1997;77:359-396.

2 Alvarez de la Rosa D, Canessa CM, Fyfe GK, Zhang P: Structure and regulation of amiloride-sensitive sodium channels. Annu Rev Physiol 2000;62:573-594.

3 Kellenberger S, Schild L: Epithelial sodium channel/degenerin family of ion channels: a variety of functions for a shared structure. Physiol Rev 2002;82:735-767.

4 Rotin D, Kanelis V, Schild L: Trafficking and cell surface stability of ENaC. Am J Physiol Renal Physiol 2001;281:F391-399.

5 Hill WG, An B, Johnson JP: Endogenously expressed epithelial sodium channel is present in lipid rafts in A6 cells. J Biol Chem 2002;277:33541-33544.

6 Hill WG, Butterworth MB, Wang H, Edinger RS, Lebowitz J, Peters KW, Frizzell RA, Johnson JP: The epithelial sodium channel (ENaC) traffics to apical membrane in lipid rafts in mouse cortical collecting duct cells. J Biol Chem 2007;282:37402-37411.

7 Balut C, Steels P, Radu M, Ameloot M, Driessche WV, Jans D: Membrane cholesterol extraction decreases Na^+ transport in A6 renal epithelia. Am J Physiol Cell Physiol 2006;290:C87-94.

8 West A, Blazer-Yost B: Modulation of basal and peptide hormone-stimulated Na transport by membrane cholesterol content in the A6 epithelial cell line. Cell Physiol Biochem 2005;16:263-270.

9 Awayda MS, Shao W, Guo F, Zeidel M, Hill WG: ENaC-membrane interactions: regulation of channel activity by membrane order. J Gen Physiol 2004;123:709-727.

10 Simons K, Ikonen E: Functional rafts in cell membranes. Nature 1997;387:569-572.

11 Hoekstra D, Maier O, van der Wouden JM, Slimane TA, van ISC: Membrane dynamics and cell polarity: the role of sphingolipids. J Lipid Res 2003;44:869-877.

12 Pike LJ: Rafts defined: a report on the Keystone Symposium on Lipid Rafts and Cell Function. J Lipid Res 2006;47:1597-1598.

13 Ikonen E, Simons K: Protein and lipid sorting from the trans-Golgi network to the plasma membrane in polarized cells. Semin Cell Dev Biol 1998;9:503-509.

14 Ikonen E: Roles of lipid rafts in membrane transport. Curr Opin Cell Biol 2001;13:470-477.

15 Brown DA, Rose JK: Sorting of GPI-anchored proteins to glycolipid-enriched membrane subdomains during transport to the apical cell surface. Cell 1992;68:533-544.

16 Pike LJ: Lipid rafts: heterogeneity on the high seas. Biochem J 2004;378:281-292.

17 Munro S: Lipid rafts: elusive or illusive? Cell 2003;115:377-388.

18 Lai EC: Lipid rafts make for slippery platforms. J Cell Biol 2003;162:365-370.

19 Ishikawa Y, Yuan Z, Inoue N, Skowronski MT, Nakae Y, Shono M, Cho G, Yasui M, Agre P, Nielsen S: Identification of AQP5 in lipid rafts and its translocation to apical membranes by activation of M3 mAChRs in interlobular ducts of rat parotid gland. Am J Physiol Cell Physiol 2005;289:C1303-1311.

20 Kowalski MP, Pier GB: Localization of cystic fibrosis transmembrane conductance regulator to lipid rafts of epithelial cells is required for Pseudomonas aeruginosa-induced cellular activation. J Immunol 2004;172:418-425.

21 Toselli M, Biella G, Taglietti V, Cazzaniga E, Parenti M: Caveolin-1 expression and membrane cholesterol content modulate N-type calcium channel activity in NG108-15 cells. Biophys J 2005;89:2443-2457.

22 Li X, Galli T, Leu S, Wade JB, Weinman EJ, Leung G, Cheong A, Louvard D, Donowitz M: Na^+-H^+ exchanger 3 (NHE3) is present in lipid rafts in the rabbit ileal brush border: a role for rafts in trafficking and rapid stimulation of NHE3. J Physiol 2001;537:537-552.

23 Welker P, Bohlick A, Mutig K, Salanova M, Kahl T, Schluter H, Blottner D, Ponce-Coria J, Gamba G, Bachmann S: Renal Na^+-K^+-$2Cl^-$ cotransporter activity and vasopressin-induced trafficking are lipid raft-dependent. Am J Physiol Renal Physiol 2008;295:F789-802.

24 Yarbrough TL, Lu T, Lee HC, Shibata EF: Localization of cardiac sodium channels in caveolin-rich membrane domains: regulation of sodium current amplitude. Circ Res 2002;90:443-449.

25 Shibata EF, Brown TL, Washburn ZW, Bai J, Revak TJ, Butters CA: Autonomic regulation of voltage-gated cardiac ion channels. J Cardiovasc Electrophysiol 2006;17 Suppl 1:S34-S42.

26 Martens JR, O'Connell K, Tamkun M: Targeting of ion channels to membrane microdomains: localization of K_V channels to lipid rafts. Trends Pharmacol Sci 2004;25:16-21.

27 Christian AE, Haynes MP, Phillips MC, Rothblat GH: Use of cyclodextrins for manipulating cellular cholesterol content. J Lipid Res 1997;38:2264-2272.

28 Loffing J, Korbmacher C: Regulated sodium transport in the renal connecting tubule (CNT) via the epithelial sodium channel (ENaC). Pflügers Arch 2009;458:111-135.

29 Rossier BC, Stutts MJ: Activation of the epithelial sodium channel (ENaC) by serine proteases. Annu Rev Physiol 2009;71:361-379.

30 Lang F, Bohmer C, Palmada M, Seebohm G, Strutz-Seebohm N, Vallon V: (Patho)physiological significance of the serum- and glucocorticoid-inducible kinase isoforms. Physiol Rev 2006;86:1151-1178.

31 Diakov A, Korbmacher C: A novel pathway of epithelial sodium channel activation involves a serum- and glucocorticoid-inducible kinase consensus motif in the C terminus of the channel's alpha-subunit. J Biol Chem 2004;279:38134-38142.

32 Lee IH, Campbell CR, Song SH, Day ML, Kumar S, Cook DI, Dinudom A: The activity of the epithelial sodium channels is regulated by caveolin-1 via a Nedd4-2-dependent mechanism. J Biol Chem 2009;284:12663-12669.

33 Hanwell D, Ishikawa T, Saleki R, Rotin D: Trafficking and cell surface stability of the epithelial Na^+ channel expressed in epithelial Madin-Darby canine kidney cells. J Biol Chem 2002;277:9772-9779.

34 Prince LS, Welsh MJ: Cell surface expression and biosynthesis of epithelial Na^+ channels. Biochem J 1998;336 (Pt 3):705-710.

35 Canessa CM, Merillat AM, Rossier BC: Membrane topology of the epithelial sodium channel in intact cells. Am J Physiol 1994;267:C1682-1690.

36 Firsov D, Schild L, Gautschi I, Merillat AM, Schneeberger E, Rossier BC: Cell surface expression of the epithelial Na channel and a mutant causing Liddle syndrome: a quantitative approach. Proc Natl Acad Sci U S A 1996;93:15370-15375.

37 Masilamani S, Kim GH, Mitchell C, Wade JB, Knepper MA: Aldosterone-mediated regulation of ENaC alpha, beta, and gamma subunit proteins in rat kidney. J Clin Invest 1999;104:R19-23.

38 Konstas AA, Koch JP, Tucker SJ, Korbmacher C: Cystic fibrosis transmembrane conductance regulator-dependent up-regulation of Kir1.1 (ROMK) renal K^+ channels by the epithelial sodium channel. J Biol Chem 2002;277:25377-25384.

39 Wielputz MO, Lee IH, Dinudom A, Boulkroun S, Farman N, Cook DI, Korbmacher C, Rauh R: (NDRG2) stimulates amiloride-sensitive Na^+ currents in Xenopus laevis oocytes and fisher rat thyroid cells. J Biol Chem 2007;282:28264-28273.

40 Kraus C, Reis A, Naehrlich L, Dotsch J, Korbmacher C, Rauh R: Functional characterization of a novel CFTR mutation P67S identified in a patient with atypical cystic fibrosis. Cell Physiol Biochem 2007;19:239-248.

41 Rauh R, Dinudom A, Fotia AB, Paulides M, Kumar S, Korbmacher C, Cook DI: Stimulation of the epithelial sodium channel (ENaC) by the serum- and glucocorticoid-inducible kinase (Sgk) involves the PY motifs of the channel but is independent of sodium feedback inhibition. Pflügers Arch 2006;452:290-299.

42 Diakov A, Bera K, Mokrushina M, Krueger B, Korbmacher C: Cleavage in the g-subunit of the epithelial sodium channel (ENaC) plays an important role in the proteolytic activation of near-silent channels. J Physiol 2008;586:4587-4608.

43 Smart EJ, Ying YS, Mineo C, Anderson RG: A detergent-free method for purifying caveolae membrane from tissue culture cells. Proc Natl Acad Sci U S A 1995;92:10104-10108.

44 Michlig S, Harris M, Loffing J, Rossier BC, Firsov D: Progesterone down-regulates the open probability of the amiloride-sensitive epithelial sodium channel via a Nedd4-2-dependent mechanism. J Biol Chem 2005;280:38264-38270.

45 Curcio CA, Millican CL, Bailey T, Kruth HS: Accumulation of cholesterol with age in human Bruch's membrane. Invest Ophthalmol Vis Sci 2001;42:265-274.

46 Kleyman TR, Carattino MD, Hughey RP: ENaC at the Cutting Edge: Regulation of Epithelial Sodium Channels by Proteases. J Biol Chem 2009;284:20447-20451.

47 Svenningsen P, Bistrup C, Friis UG, Bertog M, Haerteis S, Krueger B, Stubbe J, Jensen ON, Thiesson HC, Uhrenholt TR, Jespersen B, Jensen BL, Korbmacher C, Skøtt O: Plasmin in nephrotic urine activates the epithelial sodium channel. J Am Soc Nephrol 2009;20:299-310.

48 Harris M, Garcia-Caballero A, Stutts MJ, Firsov D, Rossier BC: Preferential assembly of epithelial sodium channel (ENaC) subunits in *Xenopus* oocytes: role of furin-mediated endogenous proteolysis. J Biol Chem 2008;283:7455-7463.

49 Wei SP, Li XQ, Chou CF, Liang YY, Peng JB, Warnock DG, Ma HP: Membrane tension modulates the effects of apical cholesterol on the renal epithelial sodium channel. J Membr Biol 2007;220:21-31.

50 Prince LS, Welsh MJ: Effect of subunit composition and Liddle's syndrome mutations on biosynthesis of ENaC. Am J Physiol 1999;276:C1346-1351.

51 Schuck S, Honsho M, Ekroos K, Shevchenko A, Simons K: Resistance of cell membranes to different detergents. Proc Natl Acad Sci U S A 2003;100:5795-5800.

52 Wang J, Zhang ZR, Chou CF, Liang YY, Gu Y, Ma HP: Cyclosporine stimulates the renal epithelial sodium channel by elevating cholesterol. Am J Physiol Renal Physiol 2009;296:F284-290.

53 Shimkets RA, Lifton R, Canessa CM: In vivo phosphorylation of the epithelial sodium channel. Proc Natl Acad Sci USA 1998;95:3301-3305.

54 Chigaev A, Lu G, Shi H, Asher C, Xu R, Latter H, Seger R, Garty H, Reuveny E: In vitro phosphorylation of COOH termini of the epithelial Na^+ channel and its effects on channel activity in *Xenopus* oocytes. Am J Physiol Renal Physiol 2001;280:F1030-1036.

55 Becchetti A, Malik B, Yue G, Duchatelle P, Al-Khalili O, Kleyman TR, Eaton DC: Phosphatase inhibitors increase the open probability of ENaC in A6 cells. Am J Physiol Renal Physiol 2002;283:F1030-1045.

56 Shi H, Asher C, Chigaev A, Yung Y, Reuveny E, Seger R, Garty H: Interactions of beta and gamma ENaC with Nedd4 can be facilitated by an ERK-mediated phosphorylation. J Biol Chem 2002;277:13539-13547.

57 Schermer B, Benzing T: Lipid-protein interactions along the slit diaphragm of podocytes. J Am Soc Nephrol 2009;20:473-478.

58 Morrow IC, Parton RG: Flotillins and the PHB domain protein family: rafts, worms and anaesthetics. Traffic 2005;6:725-740.

59 Huber TB, Schermer B, Muller RU, Hohne M, Bartram M, Calixto A, Hagmann H, Reinhardt C, Koos F, Kunzelmann K, Shirokova E, Krautwurst D, Harteneck C, Simons M, Pavenstadt H, Kerjaschki D, Thiele C, Walz G, Chalfie M, Benzing T: Podocin and MEC-2 bind cholesterol to regulate the activity of associated ion channels. Proc Natl Acad Sci USA 2006;103:17079-17086.

60 Huber TB, Schermer B, Benzing T: Podocin organizes ion channel-lipid supercomplexes: implications for mechanosensation at the slit diaphragm. Nephron Exp Nephrol 2007;106:e27-31.

61 Plant PJ, Lafont F, Lecat S, Verkade P, Simons K, Rotin D: Apical membrane targeting of Nedd4 is mediated by an association of its C2 domain with annexin XIIIb. J Cell Biol 2000;149:1473-1484.

62 Soundararajan R, Melters D, Shih IC, Wang J, Pearce D: Epithelial sodium channel regulated by differential composition of a signaling complex. Proc Natl Acad Sci USA 2009;106:7804-7809.

63 Rizzo MA, Kraft CA, Watkins SC, Levitan ES, Romero G: Agonist-dependent traffic of raft-associated Ras and Raf-1 is required for activation of the mitogen-activated protein kinase cascade. J Biol Chem 2001;276:34928-34933.

64 Verghese GM, Gutknecht MF, Caughey GH: Prostasin regulates epithelial monolayer function: cell-specific Gpld1-mediated secretion and functional role for GPI anchor. Am J Physiol Cell Physiol 2006;291:C1258-1270.

65 Pochynyuk O, Bugaj V, Stockand JD: Physiologic regulation of the epithelial sodium channel by phosphatidylinositides. Curr Opin Nephrol Hypertens 2008;17:533-540.

66 Martin TF: $PI(4,5)P_2$ regulation of surface membrane traffic. Curr Opin Cell Biol 2001;13:493-499.